Astroparticle Physics 69 (2015) 24–29

Contents lists available at ScienceDirect

Astroparticle Physics

journal homepage: www.elsevier.com/locate/astropart

Modeling ionization and recombination from low energy nuclear recoils in liquid argon

M. Foxe [a,b,c,*], C. Hagmann [b], I. Jovanovic [a], A. Bernstein [b], T.H. Joshi [d,b,1], K. Kazkaz [b], V. Mozin [b], S.V. Pereverzev [b], S. Sangiorgio [b], P. Sorensen [b]

[a] Department of Mechanical and Nuclear Engineering, The Pennsylvania State University, University Park, PA 16802, USA
[b] Lawrence Livermore National Laboratory, Livermore, CA 94550, USA
[c] Pacific Northwest National Laboratory, Richland, WA 99352, USA
[d] Department of Nuclear Engineering, University of California, Berkeley, CA 94720, USA

ARTICLE INFO

Article history:
Received 22 December 2014
Received in revised form 12 March 2015
Accepted 20 March 2015
Available online 27 March 2015

Keywords:
Liquid argon
Ionization yield
Neutrino
Dark matter

ABSTRACT

Coherent elastic neutrino-nucleus scattering (CENNS) is an as-yet undetected, flavor-independent neutrino interaction predicted by the Standard Model. Detection of CENNS could offer benefits for detection of supernova and solar neutrinos in astrophysics, or for detection of antineutrinos for nuclear reactor monitoring and nuclear nonproliferation. One challenge with detecting CENNS is the low energy deposition associated with a typical CENNS nuclear recoil. In addition, nuclear recoils result in lower ionization yields than those produced by electron recoils of the same energy. While a measurement of the nuclear recoil ionization yield in liquid argon in the keV energy range has been recently reported, a corresponding model for low-energy ionization yield in liquid argon does not exist. For this reason, a Monte Carlo simulation has been developed to predict the ionization yield at sub-10 keV energies. The model consists of two distinct components: (1) simulation of the atomic collision cascade with production of ionization, and (2) the thermalization and drift of ionization electrons in an applied electric field including local recombination. As an application of our results we report updated estimates of detectable ionization in liquid argon from CENNS at a nuclear reactor.

1. Introduction

Dual-phase noble element detectors are extensively used in the search for dark matter [1–7], but they are also of great interest in the quest to detect coherent elastic neutrino-nucleus scatter (CENNS) [8,9]. The reasons for their extensive use include the scalability, high sensitivity [10,11], favorable electron drift properties [12,13], and relatively low cost for a dual-phase xenon (Xe) or argon (Ar) detector. It is important to understand that we are nearing the absolute limits of sensitivity of those detectors, i.e. detection of very few electron–ion pairs and photons produced by primary interaction. In addition, recoiling nuclei (or ions) transfer a large fraction of their energy to heat, in contrast to ionization by electrons, where most of the energy is expended on ionization and photon production. Therefore, an understanding of physical processes involved in detector operation at low energies is becoming increasingly important.

A variety of models have been used in the past in an effort to predict the ionization yield (defined as the number of electrons produced per energy deposited) at low energies (keV) in liquid noble element detectors. The Lindhard theory [14,15] is successful in predicting the ionization yield at higher energies (MeV), but requires an independent knowledge of the ratio of energies expended to ionization and scintillation at lower energies [16], and an additional semi-empirical proportionality factor is needed to reconcile it with the measurements. Other semi-empirical models have been constructed, aimed at predicting the nuclear quench factors and scintillation yields in a variety of scintillator materials including noble liquids [17–19]. While capable of producing good fits to the experimental detector response data, those models ignore specific reconstruction of the spatial structure of ionization tracks at low energies.

An atomistic Monte Carlo model has been previously developed to predict the nuclear quench factor in liquid argon (LAr) [8] at energies relevant for CENNS experiments conducted using antineutrinos produced by nuclear reactors. In this current work, we refine

* Corresponding author at: Pacific Northwest National Laboratory, Richland, WA 99352, USA.
E-mail address: Michael.Foxe@pnnl.gov (M. Foxe).
[1] Present address: Lawrence Berkeley National Laboratory, 1 Cyclotron Road, Berkeley, CA 94720, USA.

http://dx.doi.org/10.1016/j.astropartphys.2015.03.005
0927-6505/

the atomistic Monte Carlo model [8] by including Ar^+ cross sections and the effects of local recombination in an applied drift field [20]. Though we do not estimate final uncertainties on quantitative predictions, our modeling accurately describes qualitative features of the ionization tracks at low energies which need to be taken into account in existing empirical models.

In addition to the expected ionization yields for nuclear recoil energies up to ~10 keVr, we present a revised prediction for the CENNS ionization yields produced from reactor antineutrinos.

2. Primary ionization yield using atomic collision Monte Carlo simulation

The algorithm used in the TRansport of Ions in Matter (TRIM) [21]-based binary collision Monte Carlo model has been described in previous work [8]. It handles the elastic Coulomb deflections of the incident fast Ar atom in the medium during slowing down. For the energy range considered here, most of the energy in the slowing down process is transferred to other atoms in elastic Coulomb collisions, thus dominating the stopping power $-dE/dx$. The remainder of the energy is transferred through inelastic collisions.

In this work we have included the ionization and excitation of a neutral Ar atom by another Ar atom or Ar^+ ion and charge exchange between a fast Ar^+ ion and a neutral background Ar atom. Figs. 1 and 2 show the inelastic cross sections compiled by Phelps [22] for incident Ar and Ar^+ projectiles, respectively. All ionization and excitation cross sections are small compared to the geometric cross section $\sigma_{geo} = n^{-2/3}$ for elastic Coulomb deflections, where n is the Ar number density [8,21].

The excitation producing 811 and 795 nm photons is ignored for this simulation. The 811 nm and 795 nm cross sections are 10% and 2.5% of the ionization/UV cross section, respectively [22]. For a 10 keV recoil, it is estimated that <100 eV would be lost to the production of 811 and 795 nm photons.

We take the probability for ionization occurring in a Coulomb collision as $p_{ion} = \sigma_{ion}/\sigma_{geo}$, where σ_{ion} is the ionization cross section; an analogous expression is used for excitation. In every Coulomb collision the inelastic channels are sampled based on those probabilities and are uncorrelated with the scattering angle. One of the outgoing particles is randomly chosen to be Ar^+ for ionization events and similarly Ar^* for excitations. Due to the large charge transfer cross section, σ_{CT}, few Ar^+ atoms survive to the next collisions event, with a survival probability estimated as

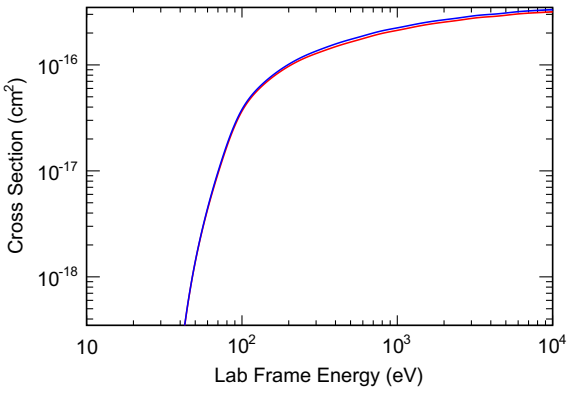

Fig. 1. In a given neutral–neutral (Ar + Ar) collision, elastic scattering, ionization, or excitation can occur. Shown are the cross sections for ionization (red), $Ar + Ar \rightarrow Ar + Ar^+ + e^-$, and excitation (blue), $Ar + Ar \rightarrow Ar + Ar^*$, based on tabulated values in Ref. [22]. The cross sections are nearly equal, with excitation cross section being slightly higher than ionization cross section, which results in similar rates of primary excitation and ionization. (For interpretation of the references to color in this figure legend, the reader is referred to the web version of this article.)

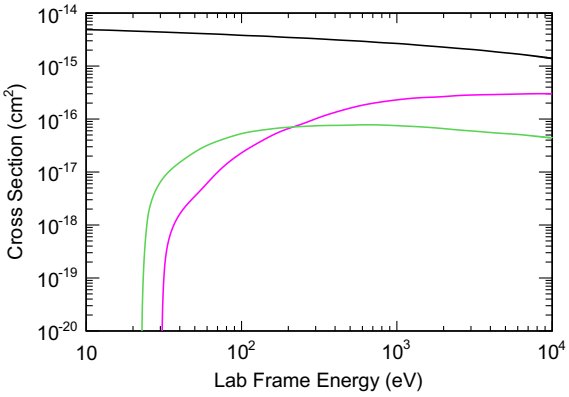

Fig. 2. Cross sections for charge transfer (black), $Ar^+ + Ar \rightarrow Ar + Ar^+$, ionization (magenta), $Ar^+ + Ar \rightarrow Ar^+ + Ar^+ + e^-$, and excitation (green), $Ar^+ + Ar \rightarrow Ar^*$, based on tabulated values in Ref. [22]. (For interpretation of the references to color in this figure legend, the reader is referred to the web version of this article.)

$p_{sur} = \exp(-\sigma_{CT}/\sigma_{geo})$. The leading particle plus all secondaries with kinetic energies larger than the excitation or ionization threshold (~25 eV in the laboratory frame) are tracked as a part of the collision cascade.

Other approximations made include: (1) the inelastic cross sections of a fast Ar^* atom are taken to be the same as an Ar atom in the ground state due to the lack of data, and (2) the target atom in a collision is assumed to be a neutral Ar in the ground state. The additional energy lost in an inelastic collision is taken from the more energetic outgoing particle to eliminate the possibility of a particle acquiring negative energy.

Unfortunately, the experimental uncertainties of the cross sections used in this simulation are not known. Also, while the TRIM algorithm is often used for problems similar to the one considered here, we are unaware of a solid treatment in the literature of systematic uncertainties arising from neglecting three-body collisions in modeling ionization dynamics in liquid.

The ionization electron spectrum is not well known and evidence exists that it depends on the collision energy [23]. For our studies of electron drift and recombination, we chose two discrete electron energies, $E_{elec} = 3$ and 10 eV, based on the electron spectrum for Ar–Ar collisions in Ref. [23]. Material-specific input parameters taken into account in the simulation are listed in Table 1, and a summary of all treated interactions is provided in Table 2.

The range of Ar atoms with keV energies in LAr, shown in Fig. 3, is short compared to the range of electrons of the same energy. The Ar ion recoil is simulated in this work, while electron recoils have been previously simulated in [20].

The primary ionization yields were obtained by averaging 10000 collision histories for each incident energy. The positions of the Ar ionization sites were recorded for the recombination stage of the simulation. Fig. 4 shows the average number of produced ionization electrons as well as their dispersion which affects energy resolution. The ionization yield is only slightly (~2%) larger

Table 1
Material specific properties of LAr used in the atomic collision model.

Property	Variable	Value	Units
Atom density	n	2.11×10^{22}	cm^{-3}
Coll. path length	L_{geo}	3.62	Å
Geo. cross section	σ_{geo}	1.31×10^{-15}	cm^2
Ionization potential	I_p	14.3	eV
Excitation energy	E_{exc}	12	eV
Ion. elec. energy	E_{elec}	3,10	eV